Theor Chem Acc (2006) 115: 145–160
DOI 10.1007/s00214-005-0051-7

REGULAR ARTICLE

Valerie Vallet · Peter Macak · Ulf Wahlgren
Ingmar Grenthe

Actinide chemistry in solution, quantum chemical methods and models

Received: 12 May 2005 / Accepted: 12 July 2005 / Published online: 13 January 2006

Abstract Theoretical modeling of actinide complexes requires access to structural parameters, information on electronic, vibration and rotation energy levels and thermodynamics properties. This article presents a critical review of theoretical studies of actinide chemistry in gas-phase and in solution and a comparison with experimental data in order to assess the applicability and accuracy by which various electronic structure theories can predict the required quantities. The quality of the basis set, the importance of electron correlation, the description of solute-solvent interactions is discussed in some detail.

1 Introduction

Actinide chemistry, like most experimental sciences, rests on a fundament of methods, data and models; it is the successful combination of these on relevant problems that leads to chemical insights. This review will focus on the use of quantum chemical methods to investigate the physical chemical properties of actinide complexes in gas phase and solution, in particular their structure and thermodynamics, both essential for the understanding of reaction mechanisms. Reactions of two different types will be discussed; the first exemplified by the gas phase reaction

$$2UO_3 + UF_6 \rightarrow 3UO_2F_2, \quad (1)$$

and the second by complex formation and the exchange of a ligand between the first and second coordination spheres

$$[UO_2(OH_2)_5], (H_2O^*) \rightarrow [UO_2(O^*H_2)_5], (H_2O), \quad (2)$$

Reaction (1) involves the breaking and formation of strong bonds and large changes in the structure between reactants and products; this is a much more difficult problem to treat accurately using quantum chemical methods than that exemplified by reaction (2), where weak labile bonds are broken / formed. The methods used to treat these two reaction types are very different and we will demonstrate this by scrutinizing theoretical methods and models based on recent computational work in molecular actinide chemistry. Whenever possible, comparisons are drawn with experimental data, to assess the accuracy of theoretical methods and discuss the applicability of chemical models.

Quantum chemistry applied to actinides should be based on "first principles" and the solution of the (time-independent) Schrödinger equation. In principle, it provides information on all chemical and physical properties of a particular compound and of its possible reactions. Quantum chemical calculations of actinide complexes of chemical relevance require appreciable computational resources because of the large number of valence electrons on the actinide center and the ligands in the first coordination sphere. The practical solution of the Schrödinger equation requires approximations that may have a bearing on the accuracy of the predictions of geometries and energy. The most important approximations that will be discussed are: (a) the choice of the relativistic Hamiltonian and the basis set, (b) the treatment of correlation effects,

Valerie Vallet (✉)
Laboratoire PhLAM, UMR CNRS 8523,
Centre d'Etudes et de Recherche Lasers et Applications,
Université des Sciences et Technologies de Lille,
F-59655 Villeneuve d'Ascq, France
E-mail: valerie.vallet@univ-lille1.fr

Peter Macak
AlbaNova University Center, Institute of Biotechnology,
Royal Institute of Technology, Roslagstullsbacken 21,
S-10691 Stockholm, Sweden
E-mail: pemac@theochem.kth.se

Ulf Wahlgren
AlbaNova University Center, Institute of Physics,
Stockholm University, Roslagstullsbacken 21,
S-10691 Stockholm, Sweden
E-mail: uw@physto.se

Ingmar Grenthe
Department of Chemistry, Inorganic Chemistry,
Royal Institute of Technology (KTH),
Teknikringen 36, S-10044 Stockholm, Sweden
E-mail: ingmarg@kth.se

(c) spin-orbit coupling and (d) solute-solvent interactions. It is necessary to strike a balance between the level of detail in the quantum chemical method used and the accuracy required; the more details and the higher the accuracy, the longer the computation time and the larger the cost. The total energy of a certain chemical species is much larger than the energy of chemical reactions and its accuracy varies significantly with the quantum chemical methods used. The situation is different for bond distances that in general vary less than 0.1 Å between different methods. More important than the accuracy in predicting absolute values for bond distances and energies is the fact that systematic errors often remain essentially constant and therefore cancel out to a large extent, e.g. when comparing the geometry of different isomers or when computing the energy of a chemical reaction. The latter aspect is very important when benchmarking methods and designing the chemical models where the quantum chemical methods will be applied.

2 Computational methods

The high nuclear charge of actinide elements makes it necessary to take relativistic effects into account, in order to give an accurate representation of their electronic structure. In quantum chemistry, the relativistic Dirac equation is the most exact way of including these effects. The four-component Dirac equation is fairly complicated, but it can be brought to a two- component form by the Douglas–Kroll–Hess transformation [1, 2]. A scalar form of the relativistic Hamiltonian, which is only marginally more complicated than the normal non-relativistic Hamiltonian, is obtained by removing the spin-dependence. Based on the relativistic spin-free Hamiltonian spin-orbit effects can be calculated within the LS coupling scheme either at the variation-perturbation level using selected spin-free states as a basis like in the RASSI module [3] of the Molcas program package [4], or at the spin-orbit CI level with the EPCISO program [5]. A very efficient method for calculating spin orbit integrals is provided by the mean-field method [6, 7]. However, the large number of electrons still makes the calculations fairly time-consuming. One can replace the computationally demanding yet chemically unimportant core electrons by potential functions that are designed to mimic their effects on the valence electron density, at the same time as they take their relativistic nature into account. In lighter elements, such as the transition metals or the lanthanides, it is well known that Effective Core Potentials (ECP) that include the outer core orbitals in the valence shell are of essentially the same quality as their all-electron counterparts. The 6*s* and the 6*p* orbitals in the early actinides are much more flexible than their counterparts in the transition metals or the lanthanides, in which they would be considered as (outer) core orbitals. The semi-valence character of the 6*s* and the 6*p* orbitals was first pointed out by Pyykkö [8], who introduced the concept of a 6*p* hole, which implies that an electron is excited into the outer valence shell and thereby active in bond formation. This makes the choice of the core in the ECP somewhat delicate for the early actinides. In the energy-consistent ECPs for actinides developed by the Stuttgart group [9, 10] the core was chosen to comprise the 1*s*-4*s*, 2*p*-4*p*, 3*d*-4*d* and the 4*f* shells, leaving 32 electrons in the valence shell for uranium. Ismail et al. [11] observed that the ECP results did not become stable for uranyl(VI), until the valence space was increased to include 32 electrons. Several studies by Vallet et al. [12], García-Hernández et al. [13], Batista et al. [14] and Straka and Kaupp [15] have shown that small core ECPs yield accurate results for geometries and energies; the bond distances come out slightly too long, up to 0.02 Å in the uranyl ion [12]. However, the large core ECPs from Hay and Martin [16–19] are less accurate, a fact noted also by Tsushima et al. [20].

At the Density Functional Theory (DFT) level, a large core ECP and the BP functional yields a bent uranyl(VI) structure with a O–U–O angle of 153°. This implies that the large core ECPs may not be suitable for the description of the valence shells of early actinides.

The choice of method to treat correlation is another problem, which is also connected with the semi-valence behavior of the outer core in the early actinides. The coupled cluster CCSD [21] and CCSD(T) [22, 23] methods are both size consistent and highly accurate, but in the coupled cluster methods only single determinant reference states can be used. However, actinide complexes with 2–12 unpaired 5*f* electron are usually multi-configurational due to atomic angular momentum coupling, and must be treated with multi-reference methods. Conventional multi-reference singles and doubles CI methods are vulnerable to size-consistency errors. The Davidson correction [24] is normally used in such calculations for systems with more than 10 electrons; however, for systems with more than 20 electrons the results often become unreliable. Somewhat larger systems can be treated using ACPF [25], a method that is essentially an iterative Davidson procedure where the number of electrons that can be correlated is still quite limited. CASPT2 [26, 27] is applicable, but in order to attain accurate results a large, preferably full, valence space must be used; this is for practical purposes essentially impossible even for "small" complexes such as the hydrated UO_2^{2+} ion with a saturated first hydration shell. A remaining possibility is to use minimal CASPT2 with one or a few strongly coupled *f*-configurations in the reference space; for all practical purposes this is equivalent to MP2 and will be usually referred to as such in the following. All the approaches quoted so far, except MP2, are expensive and thus limited to smaller systems. The recent development of resolution of identity techniques [28, 29], combined with the MP2 method, also makes it possible to optimize the geometry of larger actinide complexes at the correlated MP2 level for the same computational cost as in a HF geometry optimization. DFT based methods, such as B3LYP [29], could also be an alternative for some actinide systems, provided that the multi-reference effects are similar for the systems under study. This is most likely the case for reactions where the oxidation state of the actinide is unchanged as in complex formation and ligand exchange reactions, although there are exceptions as discussed

below. There is a possibility that the multi-reference character might be quenched in an unrestricted DFT calculation, but this has not yet been investigated.

A third problem in quantum chemical calculations concerns the basis sets where *g* functions can be expected to be important both if the 5*f*-shell is occupied, in particular at the correlated level, but also for systems like U(VI) and Np(VII), where the 5*f*-shell is formally unoccupied but where the 5*f* orbitals participate actively in the bonding.

3 Solvent models

3.1 Equilibrium models

An important part of this review concerns chemical reactions in solution. For a general review on the solvent models applied in quantum chemistry cf. the Tomasi and Persico [31], and Cramer and Truhlar [32] and references therein. Solvation effects can be modeled by including a few hundred discrete solvent molecules in the model or by describing the solutes as clusters embedded in a dielectric continuum. In the latter model the solvent is usually assumed homogeneous and isotropic and characterized by a scalar, dielectric constant. This model assumes a linear response of the solvent to a perturbing electric field. However, it was early recognized that the quantitative applicability of this model was limited by the specific interactions of the solute with solvent molecules in the region close to the solute where the solvent has properties different from the bulk; the first solvation shell dominates these effects. It is therefore important to use a complete first coordination sphere before embedding the solute in the solvent. The charges on the solute will induce opposite charges on the wall of the solvent cavity that will act as a first approximation to the hydrogen bond interactions between solute and solvent in real systems; hence the solvent will have some effect on bond distances in the first coordination sphere as discussed in Sect. 4. A better approximation of the hydrogen bonding in these systems is to include the solutes with specific outer solvation shells. In these so-called hybrid quantum mechanical/ molecular mechanical (QM/MM) methods [33–36], the metal ion with one or two hydration shells is treated at the QM level and the outer-spheres at the MM level. In addition, long-range interactions can be taken into account by a dielectric continuum model. It is difficult to treat a large number of solvent molecules quantum mechanically at the same level as the solute, in part because of the many possible locations and conformations of the explicit solvent molecules. It should also be emphasized that it is important to account for the electronic response in the MM region for charged systems. There are so far only few studies of solvated actinide with QM/MM methods [37]. However, calculations with "micro" solvated clusters (few water molecules) with a surrounding continuum often provide good approximations of solvation.

Another approach to the solvent problem is to use a statistical ensemble for the solvent. The models include a large number of solvent molecules and the solute-solvent system is represented by an ensemble of structural snapshots that fluctuate with time rather than by a single static geometry configuration. The exploration of this ensemble of configurations can be carried out in a time-independent stochastic approach (Monte Carlo) or using the deterministic molecular dynamics methods (MD). MD simulations on Th(IV) hydrates in aqueous solutions have been done by Yang et al. [38, 39].

A key point both in dynamics models and in QM/MM methods is the selection of reasonable interaction potentials with proper inclusion of N-body interaction among the particles of the sample [40]. It is often difficult to adjust the parameters describing the potential fields using empirical functions. An alternative is provided by ab initio molecular dynamics methods such as the Car–Parinello method [41] or QM/MM Born–Oppenheimer molecular dynamics [42]. Both use potential fields computed "on the fly", using DFT; this can also be done within a QM/MM scheme. However, these latter methods have not so far been extended to solvated actinide ions.

In the continuum models, the cavity in which the solute is immersed can be either spherical or tailored to the molecular shape. Tomasi and Persico [31] have shown that spherical cavities are well adapted for highly symmetrical molecules but inadequate for solutes with irregular shapes for which shape-adapted cavities are preferable. An example is given by Vallet et al. [43] who compared how the relative stability of two isomers of uranyl(VI) tetra fluoride complexes varied with the solvent model. One isomer was penta-coordinated with a water molecule in the first coordination sphere, $[UO_2F_4(OH_2)^{2-}]$, the other tetra-coordinated with the water molecule in the second sphere, $[UO_2F_4^{2-}]$, (H_2O). The shape of the latter complex requires a spherical cavity that is so large that the solvent effect becomes poorly described. The use of shape-adapted cavities corrects these artifacts as shown in Ref. [43]. A comparison of the shape adapted continuum model with a more detailed solvation model in which part of the outer solvation sphere was described explicitly quantum mechanically or using the hybrid QM/MM method, shows that both models correctly identifies $[UO_2F_4(OH_2)]^{2-}$ as the stable isomer. Vallet et al. used the Conductor-like Polarizable Continuum Model (CPCM) model and found the same energy difference, 10 kJ/mol, between the isomers in models with four water in the second sphere and the model that only include the first coordination sphere. Infante and Visscher [37] did not use a CPCM model and instead calculated the energy difference between isomers using up to thirty specific water molecules to describe the solvent. The energy difference between the isomers in the QM/MM model was 93 kJ/mol and in a complete QM model 59.5 kJ/mol.

3.2 Non-equilibrium solvation effects

The time scale for many chemical reactions are of the same order or slower than the time needed for the solvent to reorganize; hence the solvent can instantaneously follow the

changes of the solute charge distribution and maintain the equilibrium. However, this is not the case in reactions that involve a rapid change in the solute charge distribution and this gives rise to a solvent-solute system that is not in equilibrium; a proper solvent model must be adapted to take this into account. The Marcus model for outer-sphere electron-transfer reactions, where the solvent effect is estimated from the Marcus formula (3) includes non-equilibrium solvent effects by construction.

$$\lambda^{\mathrm{sol}} = \left(\frac{1}{2a_1} + \frac{1}{2a_2} - \frac{1}{R_{12}}\right)\left(\frac{1}{\varepsilon_\infty} - \frac{1}{\varepsilon_0}\right), \tag{3}$$

In Eq. (3) a_1 and a_2 are the radii of the cavities around the metal centers including their first hydration shells, R_{12} is the distance between them and ϵ_0 and ϵ_∞ are the static and dynamic dielectric constants of the solvent. In the Marcus model it is implicitly assumed that the complexes are fairly far apart, and the equation is therefore applicable only for outer-sphere reactions. For the inner sphere electron transfer a non-equilibrium PCM model [44] must be used, because the equilibrium model will decrease instead of increase the activation barrier. Macak et al. [45] found that the non-equilibrium PCM effect on the electron transfer barrier for inner-sphere electron transfer reactions [reactions (4), (5) and (6)]

$$\mathrm{NpO_2^{(V)}(OH)_2NpO_2^{(VI)}} \rightleftharpoons \mathrm{NpO_2^{(VI)}(OH)_2NpO_2^{(V)}}, \tag{4}$$

$$\mathrm{NpO_2^{(V)}F_2NpO_2^{(VI)}} \rightleftharpoons \mathrm{NpO_2^{(VI)}F_2NpO_2^{(V)}}, \tag{5}$$

$$\mathrm{NpO_2^{(V)}(CO_3)NpO_2^{(VI)}} \rightleftharpoons \mathrm{NpO_2^{(VI)}(CO_3)NpO_2^{(V)}}, \tag{6}$$

was small, between 1.5 and 8 kJ/mol [45]. They also showed that simplified models of the binary complexes with only one or two ligands in the first hydration sphere perform very similarly to the models with a complete first coordination sphere. The difference between models with only double hydroxide or double fluoride bridges in the first coordination sphere and those with six additional water ligands was only 1–3 kJ/mol.

For the outer sphere electron transfer the charge is transferred over considerable distance, which results in larger changes of dipole moment of the system and therefore also in larger changes of the solvent polarization. The solvent effect on the activation barrier is therefore expected to be larger, as can also be seen from the distance dependence of the solvent contribution to the reorganization energy in Eq. (3). The Marcus equation (3) gives a contribution of about 20 kJ/mol to the barrier for the outer sphere electron self exchange in uranyl and neptunyl solutions. However, if the non-equilibrium model is used on the separate complexes with filled first hydration spheres, the calculated solvent effect is more than twice as large. The large overestimate of the solvent effect on the outer sphere electron transfer barrier by the non-equilibrium PCM is most likely caused by the large unbalanced changes in the solvent polarization due to the change of charge state on the separate V and VI complexes.

3.3 Solvation energies in chemical reactions

The solvation energy, as determined by the difference in absolute energy in gas phase and solvent, is much larger than the corresponding reaction energies and the calculation of the latter only makes sense if the systematic error resulting from the simplified solution model is similar for reactants and products and therefore compensate one another in the reaction energy. The following example shows how different chemical models and calibration procedures can be used to investigate if this is the case, or not:

$$\mathrm{Zn(OH_2)_6^{2+} + NH_3 \rightarrow Zn(NH_3)(OH_2)_5^{2+} + H_2O}, \tag{7}$$

The Gibbs energy of reaction calculated from the total energy for each reactant and product requires accurate values of their solvation energy and there is no reason to assume that the systematic model errors will cancel since the reactants and products are very different. The parameters in the PCM model should therefore be adjusted so that the calculated solvation energy agrees with experimental values. However, these are not very precise, if they are available at all, and the resulting error in the PCM solvation energy may be therefore be substantial. Another possibility to take the solvation contribution to the reaction energy into account is to divide the chemical reaction studied into two steps as shown in Eqs. (8) and (9)

$$\mathrm{Zn(OH_2)_6^{2+} + NH_3 \rightarrow [Zn(OH_2)_6^{2+}], (NH_3)}, \tag{8}$$

$$\mathrm{[Zn(OH_2)_6^{2+}], (NH_3) \rightarrow [Zn(NH_3)(OH_2)_5^{2+}], (H_2O)}. \tag{9}$$

Reaction (8) describes the formation of an outer-sphere complex where the entering ligand is located in the second coordination sphere; the Gibbs energy of reaction for this step is small, a few kJ/mol, and can be estimated using the Fuoss equation [46, 47] to calculate the equilibrium constant for the formation of the outer-sphere complex. The Fuoss equation is based on an electrostatic model where the reactants are considered as hard spheres immersed in a dielectric continuum.

The next step, reaction (9), is then described using quantum chemical methods. As this is an intra-molecular reaction, the charge is the same for the reactant and the product; in addition both have almost the same volumes. Hence we can expect a substantial cancellation of errors in the solvation energy, as also confirmed by comparison with experimental data; the Gibbs energy of reaction for the "direct" calculation in Eq. (7) and using the two-step reaction are −41 and −16.6 kJ/mol, as compared to the experimental value −13.1 kJ/mol. The good agreement is certainly a coincidence but the example demonstrates an important principle (additional details are given by Vallet et al. [48]). Solvent effect on the geometry and relative stability of isomers will be discussed in the following section.

4 Calculation of structure parameters

4.1 Effect of basis set and correlation

Table 1 compares the geometry of the bare uranyl(VI) ion optimized at different computational levels. The small core ECP behaves well for geometries and in general results in slightly shorter (less than 0.01 Å) bond distances than in the corresponding all-electron calculations at all levels which shows that small core ECPs are reliable for the actinides. A particular problem for the actinides is that geometries optimized at the Hartree-Fock (HF) level underestimate the M–O_{yl} bond distances in actinyl complexes as compared to methods that include correlation. In the bare UO_2^{2+} ion the HF values for the U–O bond distance is 1.64 Å as compared to 1.70 Å at the CCSD(T) level. At the MP2 level the bond distance is 0.03 Å longer than those at the CCSD(T) level. The MP2 error is significant but not serious, since the difference is within the experimental error limits. Since the bond distances are underestimated at the HF level but overestimated at the MP2 level this could cause a problem in energy calculations. However, this error normally cancels, for example in ligand exchange reactions, nevertheless it is recommendable to optimize geometries and calculate energies at the same level as discussed in the section Energetics and Thermodynamics. The DFT/B3LYP U–O distance is 1.69 Å, thus close to the highly accurate CCSD(T) geometry.

For lighter elements, a lengthening of about 0.05 Å of a bond due to correlation would be a clear indication of near-degeneracy effects (a large static correlation contribution, also referred to as non-dynamical correlation, caused by the appearance of two or more nearly degenerate states, as in H_2 at large nuclear separation). Such effects are normally manifested in strong interactions between bonding and unoccupied anti-bonding orbitals. The question then arises whether the effect on the internal uranyl bond distance reflects a substantial static correlation of this type, or not. In their study Vallet et al. [12] found no indications of strong local correlation effects of this type in the analysis of the correlated wave function. A CASPT2 calculation on uranyl, with all bonding and antibonding electrons and orbitals in the active space (12 electrons in 12 orbitals) gave a wave function with coefficient 0.935 on the reference but no other dominant configuration. The conclusion is that although valence correlation is important, "traditional" static correlation caused by near degeneracies between bonding and antibonding orbitals, is *not* dominating. Additional statements on static correlation in the uranyl ion are given by Craw et al. [49]. A second question is whether the HF geometry optimization of actinyl(VI) complexes results in reliable structures and bond distances for the non-"yl" bonds, or not. We will begin with a discussion of the gas-phase geometries for the molecules MO_2F_2, $MO_2(OH)_2$, MO_3 and MF_6, where M = U, Np or Pu and then continue with a comparison of gas-phase and in-solution geometries for different uranyl(VI) complexes. In Table 2, we have compared the geometry of the molecules MO_2F_2, $MO_2(OH)_2$, MO_3 and MF_6, where M = U, Np or Pu and note that there is an increase of the U–O_{yl} distance by 0.06 Å in UO_2F_2, between the HF and B3LYP optimized geometries, as compared to 0.02 Å for the U–F distance. In UO_3 there is a significant difference between the HF and B3LYP geometries, the former has two distinctly different U–O distances, 1.745 and 1.828 Å, respectively, in the latter these distances are nearly the same, 1.81 and 1.85 Å ; this is due to electron delocalization in this compound at the B3LYP level. For UF_6 the difference in the U–F bond distance between HF and B3LYP is fairly small, 0.025 Å, with the experimental value in between.

The bond distances in the MF_6 for the series U–Pu is in good agreement with the experimental data. In UF_6 the B3LYP distance is 0.009 Å larger than the experimental value and the HF value 0.016 Å shorter, in both cases using a small core ECP. Privalov et al. [50] and Schimmelpfennig et al. [51] have compared the computed harmonic frequencies for MF_6 at the HF level using a small core ECP [9, 10] with HF and B3LYP data from Hay and Martin [19] that used a large core ECP. For the three first bending modes (T_{2u}) for U and Np, both the large- and small-core results are in good agreement with one another and with the experimental data (the average deviation is 6 cm^{-1}). The frequencies reported by Schimmelpfennig et al. [51] for Pu are of the same quality, with the exception of the E_g stretch mode, which is 100 cm^{-1} too low. The small core frequencies reported by Hay et al. were for technical reasons calculated for another state. Correlation is important for the higher frequencies for which the B3LYP data are in much better agreement with the experimental observations. The average errors increase to 30 cm^{-1} in PuF_6, presumably because DFT is not suited for describing its electronic ground state with two open f-shells. Inclusion of spin-orbit effect might also be necessary to improve the accuracy. The fact that the low frequency modes do not seem to be strongly dependent on correlation implies that this is also the case for gas phase entropies and heat capacities. It can be noted that if the computed HF frequencies are scaled with the empirical factor 0.9, the overall agreement with experiment is significantly improved (with the exception of the E_g mode in PuF_6).

Table 1 Bond distances in Å in the bare uranyl(VI) ion using different approximation levels [12]

Level	*g* functions	All-electron	RECP
HF	No	1.6518	1.6470
HF	Yes	1.6481	1.6432
ACPF	No	1.7162	1.7096
ACPF	Yes	1.7116	1.7080
MP2	Yes	1.7276	1.7316
CCSD(T)	Yes	1.7059	1.7007
B3LYP	Yes	–	1.692

4.2 Effects of the solvent in uranyl(VI) complexes

We will now discuss the calculated geometries of different uranyl(VI) complexes. Tables 3, 4 give a comparison of bond distances calculated using gas-phase (GP) HF and MP2

Table 2 Gas phase geometries for MO_2F_2, $MO_2(OH)_2$, MO_3 and MF_6 optimized at the HF or B3LYP levels, using either small core (SC) [9, 10] or large core (LC) [19] RECPs

Compound	Distances (HF)	ECP	Ref.	Distances (HF)	ECP	Ref.
UO_2F_2	U–O 1.712 U–F 2.094	SC	[50]	U–O 1.772 U–F 2.072	SC	[50]
NpO_2F_2	Np–O 1.672 Np–F 2.085	SC	[51]			
PuO_2F_2	Pu–O 1.666 Pu–F 2.076	SC	[51]			
$UO_2(OH)_2$	U–O_{yl} 1.72 U–O 2.13	SC	[50]			
$NpO_2(OH)_2$	Np–O_{yl} 1.687 Np–O 2.111	SC	[51]			
$PuO_2(OH)_2$	Pu–O_{yl} 1.673 Pu–O 2.118	SC	[51]			
UO_3	U–O_{yl} 1.745 U–O 1.828	SC	[50]	U–$O_{1,2}$ 1.81 U–O 1.853	SC	[52]
NpO_3	Np–O_{yl} 1.710 Np–O 1.796	SC	[51]			
PuO_3	Pu–O_{yl} 1.693 Pu–O 1.808	SC	[51]			
UF_6	U–F 1.985	LC	[19]	U–F 2.014	LC	[19]
	U–F 1.987	LC	[14]	U–F 2.025	LC	[14]
	U–F 1.985	SC	[14]	U–F 2.011	SC	[14]
	U–F 1.982	SC	[50]			
	U–F 1.996	Exp.	[53]			
NpF_6	Np–F 1.972	LC	[19]	Np–F 2.013	LC	[19]
	Np–F 1.950	SC	[51]	Np–F 1.991	SC	[54]
	Np–F 1.981	Exp.	[53]			
PuF_6	Pu–F 1.943	LC	[19]	Pu-F 1.985	LC	[19]
	Pu–F 1.934	SC	[51]	Pu–F 1.973	SC	[54]
	Pu–F 1.971	Exp.	[53]			

The distances are in Å

Table 3 Geometries of different isomers of UO_2^{2+} (aq) optimized at the HF or MP2 level, in gas phase (GP) or in a CPCM solvent with various basis sets on O and H atoms

Complex	Basis sets[a]	Method[b]	d(U–O_{yl})	d(U–O)	d(U–O_2)	Ref.
		EXAFS	1.78	2.41	–	[59]
$[UO_2(H_2O)_5]^{2+}$, (H_2O)	ECP2MWB/huzi	HF-GP	1.690	2.52(1)	4.38	[60]
	ECP2MWB/huzi	HF-CPCM	1.701	2.47(1)	4.31	[60]
	ECP2MWB/huzi	MP2-GP	1.779	2.48(1)	4.29	This work
	TZVP/TZVP	MP2-GP	1.776	2.47(1)	4.18	This work
$[UO_2(H_2O)_4]^{2+}$, $(H_2O)_2$	ECP2MWB/huzi	HF-GP	1.688	2.47	3.94	[60]
	ECP2MWB/huzi	HF-CPCM	1.700	2.45(1)	4.03	[60]
	ECP2MWB/huzi	MP2-GP	1.777	2.42	3.85	This work
	TZVP/TZVP	MP2-GP	1.774	2.41	3.87	This work
$[UO_2(H_2O)_6]^{2+}$	ECP2MWB/huzi	HF-CPCM	1.702	2.48× 2, 2.51× 2, 2.65× 2	–	[60]
	ECP2MWB/huzi	MP2-GP	1.782	2.48× 2, 2.49× 2, 2.69× 2	–	This work
	TZVP/TZVP	MP2/GP	1.785	2.47× 2, 2.49× 2, 2.64× 2	–	This work

Bond distances are in Å. The geometry optimizations have in general been made without symmetry restrictions and the computed bond average distances are given for brevity when the differences are less than 0.02 Å. In other cases the different bond distances are reported

[a] O basis / H basis. Oxygen ECP2MWB and TZVP basis sets are taken from Refs [55] and [56], respectively. Hydrogen Huzi (Huzinaga) and TZVP basis sets are taken from Refs [57] and [58], respectively

[b] Computational level for the geometry optimization

optimization and HF optimization in a CPCM solvent model. In some cases two different basis sets for O, the ECP2MWB basis set from Bergner et al. [55] and the TZVP basis of Schäfer et al. [56]; for H the Huzinaga basis set [57] and also the TZVP basis set [58] were used. The tables include experimental bond distances obtained from EXAFS in solution.

The data show that the bond distances do not vary significantly between the two different basis sets tested for O and H. The U–O_{yl} bond distance at the HF level in gas phase is about 0.07 Å shorter than the corresponding distance at the MP2 level. The bond distances in the equatorial plane of the first coordination sphere of the linear uranyl(VI) ion also varies slightly depending on the approximation used but the difference is less than 0.05 Å between HF-GP, MP2-GP and HF-CPCM and this difference does not seem to depend on the coordinated ligand. The distance between uranium and

Table 4 Geometries of different uranyl(VI), uranyl(V) and neptunyl(VI) complexes optimized at the HF or MP2 level in GP or in a CPCM solvent, with various basis sets on O and H atoms

Complex	Method[a]	d(U–O_{yl})	d(U–L_1)	d(U–L_2)	Ref.
[b] $[UO_2(oxalate)_2(OH_2)]^{2-}$	EXAFS	1.78	2.38[c]	2.38[c]	[63]
L_1 coord. O_{ox};L_2 coord. H_2O	HF-GP	1.73	2.39(7)	2.61	[63]
	Average distance U–L_1 and U–L_2 2.43 Å				
	HF-CPCM	1.73	2.40(2)	2.54	[63]
	MP2-GP	1.81	2.34(4)	2.59	This work
[d] $[UO_2(oxalate)_2F]^{3-}$	EXAFS	1.79	2.39	2.22	[63]
L_1 coord. O_{ox}; L_2 coord. F^-	HF-GP	1.74	2.48	2.21	[63]
	HF-CPCM	1.74	2.432(8)	2.22	[63]
	MP2-GP	1.83	2.432(4)		This work
[e] $[UO_2(oxalate)_3]^{4-}$	EXAFS	1.79	2.43, 2.39	–	[63]
L_1 coord. O_{ox}	HF-GP	1.73	2.48(2), 2.405	–	[63]
	HF-CPCM	1.73	2.427(6), 2.386	–	[63]
	MP2-GP	1.82	2.44(1), 2.355	–	This work
[f] $[UO_2F_4(OH_2)]^{2-}$	EXAFS	1.80	2.26	2.48	[43]
L_1 coord. F^- ; L_2 coord. H_2O	HF-GP	1.740	2.28(4)	2.748	[43]
	HF-CPCM	1.751	2.26(1)	2.62	[43]
	MP2-GP	1.84	2.27(4)	2.62	This work
[g] $[UO_2(OH)_4]^{2-}$	EXAFS	1.83(0)	2.26(6)	–	[43]
L_1 coord. OH^-	HF-GP	1.763	2.336	–	[43]
	HF-CPCM	1.768	2.299(1)	–	[43]
	MP2-GP	1.87	2.299	–	This work
$UO_2(CO_3)_3^{4-}$	EXAFS	1.80	2.43		[64]
	MPT2-GP	1.89_4	2.42_6		[61]
	MPT2-SCRF	1.88_1	2.40_7		[61]
	CASPT2[h]-SCRF	1.85			[61]
	HF-GP	1.75	2.55		[65]
$UO_2(CO_3)_3^{5-}$	EXAFS	1.90	2.50		[64]
	MPT2-SCRF	1.93_3	2.52_9		[61]
	CASPT2[h]-SCRF	1.93			[61]
$NpO_2(CO_3)_3^{5-}$[i]	EXAFS	1.86	2.53		[66]
	MPT2-SCRF	1.88_6	2.62_8		[62]
	CASPT20-SCRF	1.88	2.60		[62]

Bond distances are in Å. The geometry optimizations have in general been made without symmetry restrictions and the computed bond average distances and the maximum deviation from this are given for brevity. SCRF stands for Self Consistent Reaction Field Hamiltonian with spherical cavity to account for solvent effects, see Refs. [61, 62]

[a] Computational level for the geometry optimization

[b] Isomer 1 of Ref. [63]

[c] Denotes the average value between four U–O_{ox} and one U–OH_2 distance; the experimental data are not accurate enough to separate the two

[d] Isomer 1 of Ref. [63]

[e] Structure 1 of Ref. [63]

[f] Structure 1 of Ref. [43]

[g] Structure 5b of Ref. [43]

[h] Active space: 12 electrons in 12 orbitals for U; 10 electrons in 12 orbitals for Np

[i] Geometry optimised with three Na^+ counterions

water in the second coordination sphere varies slightly more with the model used, as seen in Table 3.

When comparing computed bond distances with experimental EXAFS data it is also necessary to take the accuracy of the latter into account. The analysis of EXAFS data is often straightforward and results in estimated uncertainty of bond distances of 0.01–0.02 Å. Gagliardi et al. [61] have optimized the structures of tricarbonato complexes of uranyl in the formal oxidation state VI and V and neptunyl(V) at the second-order perturbation theory level MP2 and minimal CASPT2. The computed bond distances, in particular the equatorial bond distances agree very well with experimental data [64]. The bond distances obtained for uranyl(VI) at the minimal CASPT2 level with two electrons in seven orbitals and in a CASPT2 calculation with 12 electrons in 12 orbitals are 1.88 and 1.85 Å respectively (Table 4), in agreement with the results for the bare uranyl(VI) ion (Table 1). However, for uranyl(V) the minimal-CASPT2 and the CASPT2 results are virtually the same. HF data by Pyykkö et al. [65] for the U(VI)-carbonate deviate by 0.12 Å from EXAFS data. One reason might be that Pyykkö et al. [53] used a large core ECP [16]. Gagliardi and Roos [61] have made a detailed computational study of the structures of $NpO_2(CO_3)^-$, $NpO_2(CO_3)_2^{3-}$ and $NpO_2(CO_3)_3^{5-}$ and compared the results with experimental EXAFS data from Clark et al. [66]. The agreement is in general satisfactory. However, Gagliardi and

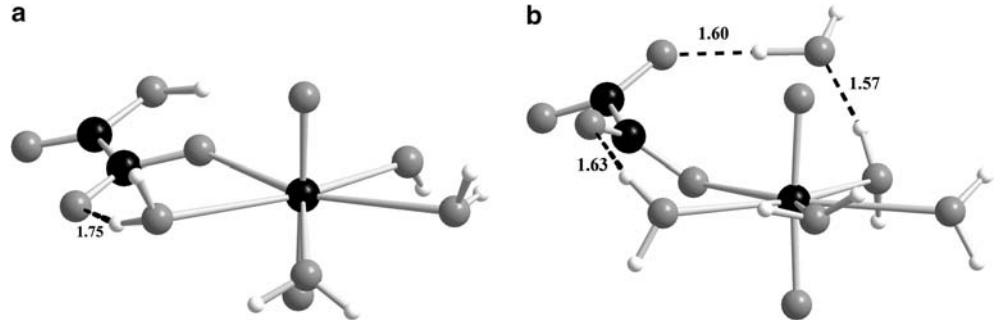

Fig. 1 Perspective views of the structures of the complexes **a** $[UO_2(\text{oxalate-uni})(H_2O)_4]$ that shows proton abstraction and **b** $[UO_2(\text{oxalate-uni})(H_2O)_4],(H_2O)$, in which a water molecule has been included in the second-sphere. Geometries have been optimized at the HF level in gas-phase. The *dashed line* indicates hydrogen bond interactions. Bond distances are in Å

Roos [61] noticed that $NpO_2(CO_3)_3^{5-}$ is not a stable species unless Na^+ counter ions are explicitly included, as compared to the corresponding uranyl(V) species. This may be due to problems arising in connection with the solvent model when there is more than one open *f*-shell on the actinide. Tsushima et al. [20] have compared the structures of $UO_2(OH_2)_5^{2+}$ and $UO_2(CO_3)_3^{4-}$ optimized at different theory levels (HF, B3LYP, MP2) using a large core ECP; they have also tested different basis sets on H and O. They find that the bond distances in the equatorial plane differ less than 0.05 Å between different theoretical models. However, their data for the tris-carbonato complex differs significantly from that of Gagliardi et al. [61] and EXAFS data. Tsushima et al. suggest that this is the result of the use of a large core ECP.

The analysis of the EXAFS data for the complexes $[UO_2(\text{oxalate})_2(OH_2)]^{2-}$ and $[UO_2(\text{oxalate})_3]^{4-}$ is not straightforward and one can only determine an average U–O distance in the first coordination sphere. The best agreement between experimental and calculated bond distances, in general 0.05 Å or better, is obtained with the MP2-GP and HF-CPCM models. In $[UO_2(\text{oxalate})_2(OH_2)]^{2-}$ there is no experimental value for the U–water distance, only an average value, 2.38 Å, for all U–O distances; also this is in good agreement with the calculated average values at the HF-CPCM level or MP2-GP levels, 2.43 and 2.39 Å, respectively. The only example where there is a larger deviation between the computed and experimental bond distances is the U–OH_2 distance in $UO_2F_4(OH_2)^{2-}$.

New codes that allow rapid geometry optimization at the MP2 level in gas-phase are now available and these give geometries that are close to the experimental values. The systematic error introduced in the U–O_{yl} distance at the HF-GP level does not result in errors in the equatorial bond distances as long as these do not involve delocalization of electrons between the metal ion and ligand as is the case in molecules like UO_3.

Other types of modeling errors can appear in gas phase geometry optimization at the HF level such as abstraction of a proton from coordinated water to another ligand in the first coordination sphere; this was encountered in $[UO_2(\text{oxalate-uni})(H_2O)_4]$, cf. Fig. 1a. This error can be avoided by adding a second coordination sphere of water that can form hydrogen bonds to the ligand in the first sphere, see structure of $[UO_2(\text{oxalate-uni})(H_2O)_4]$ in Fig. 1b.

A second type of model error has been observed when studying geometry optimization of $UO_2(OH_2)_6^{2+}$. This ion turned out to be unstable in gas phase geometry optimization at the HF level, but was stable when the optimization was made at the MP2 level or at the HF level in the CPCM solvent. The stability seems to be very sensitive both to the level of correlation and to the basis set, as discussed by Hay et al. [67]. It is important to test the stability of structures at different levels of approximation.

The effect of the geometry differences on reaction energies will be discussed in Sect. 5.

Conclusions Geometry optimization at the HF level in gas phase results in reasonable bond distances, except for covalent bonds such as the uranyl bonds. The equatorial bonds in actinyl(VI) and (V) complexes with a large ionic character are in much better agreement with experiments. Geometry optimization at the HF level in the solvent does not change the equatorial bond distances significantly for charged ligands; however the U–OH_2 distance may decrease by up to 0.12 Å, presumably as a result of hydrogen bonding. Martínez et al. [68] have discussed the influence of solute–solvent interactions on metal–ligand bond distances. In an earlier article [69], they pointed out that while short range specific interactions, mainly hydrogen bonding, shorten the metal-water bond distance, long-range interactions lengthen it, leading to a mutual partial cancellation of the effects when the two types of interactions are jointly considered. Geometry optimization at the MP2-GP level provides as expected a much better description of the covalent bonds, but bond distances for the equatorial ligands deviate at most 0.05 Å from the values obtained at the HF level (with the exception noted above).

4.3 The effect of spin-orbit coupling on geometries

Van Lenthe et al. [70] have studied the effect of spin-orbit on the ground state properties (bond distances and frequencies)

in a series of closed-shell diatomic molecules. In these systems, the spin orbit effect on the bond distance never exceeds 0.03 Å, and the effect on frequencies is less than 10%. The effect is strongest in molecules where the spin-orbit split orbitals participate actively in the bonding, like the 6*p* of Bismuth in Bi_2; this is not the case in the early actinides where the singly occupied 5f orbitals are localized on the actinide center and are non-bonding due to symmetry. García–Hernández et al. [13] have compared all-electron calculations with and without inclusion of spin-orbit coupling for various density functionals for closed-shell uranyl and UF_6, and open-shell neptunyl and NpF_6. The influence of spin-orbit coupling on geometries and vibrational frequencies is small, 0.003 Å, and 3–8 cm^{-1}, respectively. This indicates that in closed-shell actinide systems high-order spin-orbit effects can be neglected. For open-shell early actinides, spin-orbit does not influence the geometries and frequencies but should be taken into account in energy calculations as will be discussed in Sect. 5.2. This also applies to the geometry of the first excited states of the early actinide ions, which correspond either to *f-f* excitations, or charge-transfer excitations from bonding orbitals on the actinide center to non-bonding *f* orbitals ($f_\varphi f_\delta$ orbitals). Charge-transfer states have often longer axial An–L distances than pure *f* states, but bond distances agree to 0.01 Å within each category of states, and are unaffected by spin-orbit coupling. Examples can be found in the studies of electronic spectra of neptunyl(VI) and (V) by Matiska and Pitzer [74], plutonyl(VI) and PuN_2 by Clavaguéra et al. [72] and UCO by Roos et al. [73]. However, with increasing number of unpaired 5f electrons, intra-shell spin-orbit coupling mixes spin-free configurations and has to be taken into account to determine the exact nature of the ground state.

5 Energetics

In this section we will discuss the effect of correlation, basis set and solvent on the total energy of actinide complexes and the energy of complex formation reactions.

5.1 Effect of correlation and basis set

Several of these problems have been discussed by Vallet et al. [12] using the following reactions:

$$UO_2^{2+} + 1/2H_2O \rightarrow HOUO^{2+} + 1/4O_2, \quad (10)$$

$$HOUO^{2+} + 1/2H_2O \rightarrow U(OH)_2^{2+} + 1/4O_2, \quad (11)$$

$$UO_2^{2+} + H_2O \rightarrow U(OH)_2^{2+} + 1/2O_2. \quad (12)$$

Reactions (10) and (11) describe the stepwise reduction of U(VI) via U(V) to U(IV) by water and their sum reaction (12). It is well known experimentally that uranyl(VI) cannot be reduced by water, but the reaction can be used in a thermodynamic cycle in order to shed light on methodological problems; Vallet et al. [74] have used this approach and shown that good estimates of the redox potentials were obtained by studying the same sequence of reactions for Np, Pu and Am, using the U system for calibration.

Vallet et al. used the small core ECP suggested by the Stuttgart group, and investigated its accuracy, the importance of g functions in the uranium basis set and the accuracy of different correlation methods.

There is a mistake in the article by Vallet et al. [12] in the calculated energies at the HF level (the correlated results and the calculated redox potentials are correct, however). In Table 5 we present the reaction energies obtained by Vallet et al. [12] together with new HF values calculated by us. The error in the ECP compared to the all-electron results is at most 5 kJ/mol. The effect of the *g* functions on uranium at the HF level is surprisingly large, in particular for the second reaction. This result shows that the *g* functions can be important for complexes with occupied 5*f*-orbitals even at the HF level. In a test calculation on reduction of uranyl [12], the large core ECP from Hay and Martin [19] gave a reaction energy that was about 20 kJ/mol more endothermic than that obtained with the small core ECPs (35 vs. 16 kJ/mol).

It is generally assumed that high angular momentum functions are more important at the correlated level than at the HF level. As demonstrated by Vallet et al. [12] this is not necessarily true for actinide complexes, where the largest effect of the *g* functions occurs at the HF level. It should be emphasized that the reactions studied by Vallet et al. are quite complicated, involving both an electron transfer reaction and the breaking of a triple bond in the uranyl unit. The results may therefore be atypical. It is noteworthy that DFT results obtained with either hybrid (B3LYP) or pure LDA (VWN, BP) [75] functionals strongly deviate from ab initio MP2, ACPF and CCSD(T) results [12]. All three functionals predict the first reaction to be exothermic, which is inconsistent with the other results. Moreover, the pure functionals, VWN and BP, yield results that can differ by as much as 30 kJ/mol. This indicates that the present functionals cannot describe the breaking and forming of strong bonds that involve a significant rearrangement of the electron density at the actinide center.

Privalov et al. [50] have investigated the reaction energy for a number of gas phase reactions

$$2UO_3(g) + UF_6(g) \rightarrow 3UO_2F_2(g), \quad (13)$$

$$UO_2F_2(g) + 2H_2O(g) \rightarrow UO_2(OH)_2(g) + 2HF(g), \quad (14)$$

$$UF_6(g) + 2H_2O(g) \rightarrow UO_2F_2(g) + 4HF(g), \quad (15)$$

$$UO_3(g) + H_2O(g) \rightarrow UO_2(OH)_2(g), \quad (16)$$

$$UF_6(g) + 3H_2O(g) \rightarrow UO_3(g) + 6HF(g). \quad (17)$$

The correlation contribution was calculated using MP2, CCSD(T) and B3LYP.

Reactions (13), (14), (15), (16) and (17) should provide a sensitive test both on the basis set effect and the accuracy of correlation methods, since the bonds in these complexes are strong.

Schimmelpfennig et al. [51] extended this study to include the corresponding neptunium(VI) and plutonium(VI)

Table 5 Reaction energies in kJ/mol for Reactions (10) and (11) (see text) computed with all-electron or ECP basis, with or without g functions on the actinide center

Level	All-electron		RECP		Ref.
	No *g*	With *g*	No *g*	With *g*	
$UO_2^{2+} + {}^1/_2\,H_2O \rightarrow HOUO^{2+} + {}^1/_4O_2$					
HF	−29.5	−21.03	−34.56[a]	−22.60[b]	[12]
ACPF	41.48	40.68	42.40	44.45	[12]
MP2	–	57.32	46.80	51.29	[12]
CCSD(T)	–	47.60	–	49.78	[12]
B3LYP	–	–	–	−39.37	[12]
VWN	−66.9	–	–	–	[75]
BP	−39.7	–	–	–	[75]
$HOUO^{2+} + {}^1/_2\,H_2O \rightarrow U(OH)_2^{2+} + {}^1/_4O_2$					
HF	−138.98	−117.11	−144.16[c]	−118.66[d]	[12]
ACPF	8.09	23.72	11.44	23.34	[12]
MP2	–	2.39	4.53	18.10	[12]
B3LYP	–	–	–	−0.84	[12]
VWN	48.9	–	–	–	[75]
BP	30.5	–	–	–	[75]

Values taken from Ref. [12]
[a] Old value −34.56
[b] Old value −28.91
[c] Old value: −129.30
[d] Old value −91.47

Table 6 Reaction energies for the gas phase reactions (13), (14), (15), (16), (17), and (18) in kJ/mol, calculated with all-electron (AE) or RECP basis sets. ANO-L denotes the large ANO basis sets given in the Molcas package (see below)

Reaction	$2UO_3 + UF_6 \rightarrow 3UO_2F_2$	$UO_2F_2 + 2H_2O \rightarrow UO_2(OH)_2 + 2HF$	$UF_6 + 2H_2O \rightarrow UO_2F_2 + 4HF$	$UO_3 + H_2O \rightarrow UO_2(OH)_2$	$UF_6 + 3H_2O \rightarrow UO_3 + 6HF$
MP2/ECP without *g*	−278 (54)	101 (14)	232 (14)	−154 (34)	487 (−5)
MP2/ECP with *g*	−288 (44)	105 (18)	200 (−18)	−139 (49)	443 (−49)
MP2/AE with *g*	−306 (26)	86 (−1)	168 (−50)	−151 (37)	405 (−87)
CCSD(T)/ECP without *g*	−329 (3)	110 (23)	263 (45)	−186 (2)	558 (66)
CCSD(T)/ECP with *g*	−329 (3)	113 (26)	241 (23)	−172 (16)	526 (34)
B3LYP/ECP without *g*	−262 (70)	130 (43)	332 (114)	−166 (22)	627 (135)
CCSD(T)/ECP ANO-L basis	−332	87	218	−188	492

Values in parenthesis are the deviations from the CCSD(T) ANO-L results. Values taken from Refs. [50, 51]

reactions, for which experimental data are not available. They investigated both the accuracy of the correlation methods and of the small core ECPs, and noted that the *g* functions at the correlated level are important in these reactions. The medium sized basis sets used in most of the reported calculations give acceptable results, which still differ by about 20 kJ/mol different from those obtained with the large basis set CCSD(T) (Table 6).

The uncertainty connected with the different correlation methods is moderate to large. The MP2 results differ from the large CCSD(T) calculation by up to 50 kJ/mol. Reactions (14), (15) and (17) involve the formation of HF, which is difficult to describe with any correlation method. Privalov et al. [50] suggested a normalization procedure to minimize the systematic errors in the calculation. They used a constant difference between the calculated and measured reaction energies for reaction (13) and applied this to the other reactions and thereby obtained a dramatic improvement in the results compared to experiment.

A surprising feature noted by Schimmelpfennig et al. [51] is the difference between the MP2 results calculated at the ECP and the all-electron levels, which is about 10–20 kJ/mol for reactions (13), (14) and (16), and 32 and 38 kJ/mol for reactions (15) and (17). The reason is presumably the errors induced by the nodeless character of the orbitals in the ECP calculations. The B3LYP results deviate even more from the large basis CCSD(T) results, in particular for reactions (15) and (17).

In the systems studied by Vallet et al. [12], Privalov et al. [50] and Schimmelpfennig et al. [51] it is clearly important to include *g* functions in the basis set already at the HF level, and also to properly select the correlation method. Schimmelpfennig et al. [51] estimate that the uncertainty in the MP2 reaction energies is about 50 kJ/mol.

The reactions studied by Vallet et al. [12] involved both bond breaking and a change in oxidation state, while the studies by Privalov et al. [50] and Schimmelpfennig et al. [51] concerned compounds with strong bonds. As will be

Table 7 Reaction energies in kJ/mol for the *D* and *A* water exchange pathways in $[UO_2(H_2O)_5]^{2+}$ [Eqs. (18) and (19) of the text]. Geometries are optimized at the HF or MP2 level with O and H basis sets indicated in brackets (O basis/H basis)

Basis set[a]	Method for geometry optimization	Method for single-point calculation	*D*-intermediate	*A*-intermediate	Ref
6-31++G**/6-31++G**	B3LYP-GP	B3LYP-GP	−1.7	101.4	[76]
		B3LYP-PCM	20.5	98.5	
ECPTLS/DZP	B3LYP	B3LYP-GP	44.8	–	[77]
ECP2MWB/huzi	HF-GP	HF-GP	37.4	–	[60]
		MP2-GP	42.9	–	
		MP2-CPCM	65.8	–	
ECP2MWB/huzi	HF-CPCM	HF-CPCM	53.7	20.8	[60]
		MP2-CPCM	61.8	15.8	
ECP2MWB/huzi	MP2-GP	HF-GP	41.0 (40.5)	45.8 (46.3)	This work
		HF-CPCM	44.3 (43.8)	32.7 (33.1)	
		MP2-GP	38.2 (35.4)	34.0 (35.7)	
		MP2-CPCM	52.9 (51.8)	15.3 (16.7)	
TZVP/TZVP	MP2-GP	HF-GP	38.6 (38.8)	47.9 (49.4)	This work
		HF-CPCM	54.5 (55.0)	33.1 (34.7)	
		MP2-GP	33.8 (32.5)	32.4 (37.3)	
		MP2-CPCM	52.9 (52.0)	11.9 (16.9)	

Energies are calculated at the HF level or MP2 level in the GP or in the CPCM solvent model. Values in parenthesis were computed by including two g functions given in Ref. [12]

[a] O basis / H basis. Oxygen 6-31++G**, ECP2TLS, ECP2MWB, and TZVP basis sets are taken from Refs. [78], [79], [55], and [56], respectively. Hydrogen DZP, Huzi (Huzinaga), and TZVP basis sets are taken from Refs. [80], [57] and [58], respectively

seen later in this review, reactions that involve formation and breaking of weakly bound ligands in complex formation or ligand exchange / ligand substitution at actinides are much less sensitive to the choice of basis set and correlation methods.

A major problem with quantum chemical studies of actinide complexes is that the number of electrons is too large for standard CI methods such as multi-reference SDCI to be applicable (due to the size consistency problem) and that multi-reference effects in complexes with two or more occupied *f*-orbitals precludes the use of size consistent single reference methods such as CCSD(T). DFT is also a single reference method and furthermore it gives unsatisfactory results on strongly bound complexes. The only generally applicable method for these systems is thus MP2, but it is important to realize its shortcomings and compare the calculated results with experiments whenever possible. It is also of advantage if sequences of similar systems can be compared, since this minimizes the effects of systematic errors. Another possibility, used by several authors, is to calibrate the calculations to some known experimental result.

The situation is different for complex formation reactions taking place in gas phase and solvent; we will demonstrate this by comparing the energy for the reactions (18) and (19) given in Table 7, both in gas phase, at the HF and MP2 levels. The MP2 calculations have been made using either the gas-phase HF geometry with a single point MP2 on top or a complete MP2 with the MP2 optimized geometry.

$$[UO_2(OH_2)_5^{2+}], (H_2O) \rightarrow [UO_2(OH_2)_4^{2+}], (H_2O)_2 \qquad (18)$$

and

$$[UO_2(OH_2)_5^{2+}], (H_2O) \rightarrow [UO_2(OH_2)_6^{2+}]. \qquad (19)$$

The choice of basis set for the O and H atoms has a small influence on the calculated reaction energies, at most 4 kJ/mol. The same is true when adding a *g*-function to the U-basis set, cf. Table 7. The reaction energy for the dissociative reaction (18) changes very little between the different theoretical models; it is not possible to make the same comparison for the associative reaction (19) as $UO_2(OH_2)_6^{2+}$ is not a stable species if the geometry optimization is made at the HF-level. In the gas-phase, the difference between the reaction energies for (18) and (19) is only 4.2 kJ/mol. The data in Table 7 also show that the reaction energy between the isomers is not strongly dependent on the difference between the HF and MP2 geometry; the difference 13 kJ/mol, is small but not negligible. This indicates that one should use MP2 optimized geometries whenever possible, especially when comparing reactions with small energy differences.

Tsushima et al. [76] have studied UO_2^{2+} coordinated by four, five and six water molecules in the gas phase and solution, using B3LYP, large core ECPs, and the PCM model, imposing symmetry constraints. There are a number of significant discrepancies between our results, theirs and other MP2 [81] or B3LYP data [77]. One reason might be the symmetry constraints, another that they used a large core ECP; as discussed earlier by us and noted by Clavaguéra-Sarrio et al. [81], it is important to keep a small core.

It is at this point pertinent to return to the question of the accuracy of the MP2 method for actinide complexes. In a recent review article, Rotzinger [82] has discussed the accuracy of geometry optimization at different levels of computation; we agree with his statement that "The computationally fast HF calculations yield reasonable geometries" but not his subsequent statement that "geometry optimization at the HF and energy computations with MP2 are inadequate (for uranyl(VI) systems, our addition)"; his claim is not supported by the comparison of experimental and computed bond distances in Tables 3 and 4. In the same review article Rotzinger also made the following statements concerning

static correlation and the accuracy of the MP2 method in actinide(VI) complexes "In $UO_2(OH_2)_5^{2+}$, there is static electron correlation, arising from the population of σ^* (M=O) and π^*(M=O) MOs by σ(M=O) and π(M=O) electrons as in $VO(OH_2)_5^{2+}$." In the quoted reference (ref 10 in the Rotzinger paper [82]) there is no computation to support this statement, despite the fact that he correctly points out, "From the population of the natural orbitals (NOs), it can be seen if static correlation is present." Both results from previous studies [12, 49] and more recent results indicate that there is no static correlation of the near-degeneracy type in UO_2^{2+} ; as stated in Sect. 4.1 the coefficient of the leading configuration is 0.93 and there is no other dominant configuration. The largest occupation among the antibonding natural orbitals is 0.06, and the largest coefficient (except that for the leading configuration) is 0.08, which shows that while valence correlation is important it is not of the conventional near-degeneracy type, which would cause problems in an MP2 calculation. The wave function at the MP2 level is well behaved, and there is no reason to suspect any significant error in the energy due to near degeneracy effects. This is confirmed by the results obtained for the reduction of uranyl, which is a complicated reaction involving both bond breaking and electron transfer, where the agreement between the MP2 and the CCSD(T) results are within 20 kJ/mol, and the gas phase reactions (13), (14), (15), (16) and (17), where the agreement between CCSD(T) and MP2 is within 50 kJ/mol, which is satisfactory considering the number of compounds involved in the reactions. Our conclusion, in contrast to the statements of Rotzinger, is that perturbation methods such as MP2 are in general applicable to uranyl(VI) complexes, and in particular to describe reactions involving labile ligands. For other actinide complexes with two or more unpaired 5*f*-electrons multi-reference effects may become large due to atomic coupling effects, and in these cases a minimal CASPT2 with a few configurations in the reference state is appropriate as shown in several previous studies [11, 12, 50, 51, 62].

Conclusions The solvent effect of the electronic energy can be obtained either using the gas phase geometry and adding a single point PCM calculation, or by making the geometry optimization in the solvent. For actinide systems of even moderate size, the latter method can only be used at the HF level. We are therefore left with the following choices to compute reaction energies:

- To use gas-phase geometries at the HF level and add a single point MP2 and a single point PCM on top.
- To use a HF geometry optimized in the PCM and add a single point MP2 on top
- To use a gas-phase MP2 geometry and add a single point PCM on top.

The choice of method depends on the type of the chemical process involved, the accuracy required for the problem at hand, the available software and the computation cost. Recently, new software has become available that allow fast geometry optimization at the MP2 level for actinides and these should therefore be preferred.

A comparison between the MP2 and HF methods for energy calculations is of interest (the effect on geometry is discussed in Sect. 4). As seen in Table 7, the energy difference between the precursor $[UO_2(OH_2)_5^{2+}]$, (H_2O) and the intermediate $[UO_2(OH_2)_4^{2+}]$, ($H_2O)_2$ between the different optimized geometries is small, 12 kJ/mol between the gas phase HF geometry and the gas phase MP2 geometry and 8 kJ/mol between the solvent optimized HF geometry and the gas phase MP2 geometry; for the A-intermediate, the difference is only 0.5 kJ/mol. Our conclusion, in contrast to the opinion of Rotzinger, is that even the gas phase optimized geometry at the HF level provides a good estimate of reaction (and activation) energies for ligand exchange reactions. It should also be pointed out that the approximations inherent in all QM methods make it questionable to discuss energy differences between complexes that are smaller than 5–10 kJ/mol.

5.2 Spin-orbit effects on energetics

Formally, spin-orbit interaction contributes to decrease the energy of open-shell molecules. If the number and character of open-shell orbitals are the same for the reactant and the product, spin-orbit effects essentially compensate one another. This will be the case in ligand-exchange/substitution reactions for the early actinide ions. We have checked this assumption by calculating the spin-orbit effect on the reaction energy for the D and A-pathways, Eqs. (18) and (19) for the water exchange in $NpO_2(OH_2)_5^{2+}$ studied by Vallet et al. [82]. The lowering of the electronic energy by spin-orbit coupling of the five-coordinated precursor, the dissociative intermediate and associative intermediate is 32.1, 31.1 and 32.9 kJ/mol, respectively. This implies that the effect on the relative energies of the precursor and successors is small, less than 1 kJ/mol and can therefore be neglected. As noted earlier in this paper, the situation is very different for reactions that involve a significant rearrangement of the electron density at or close to the actinide center. Redox and electron-transfer reactions belong to this class.

Vallet et al. [12, 74] used the variation-perturbation method to describe the spin-orbit effect in reaction (12)

$$UO_2^{2+} + H_2O \rightarrow U(OH)_2^{2+} + 1/2O_2. \qquad (20)$$

The effect of spin-orbit coupling is larger for the products than for the reactants, leading to a lowering of the reactions energy from 67.7 kJ/mol at the spin-free level to 11.7 kJ/mol when spin-orbit was taken into account [12]. Hay et al. [67] have investigated $AnO_2(H_2O)_5^{2+}$ and $AnO_2(H_2O)_5^{+}$ for the An = U, Np and Pu at the gas-phase DFT/B3LYP level. They estimated spin-orbit effects using a semi-empirical spin-orbit operator and coupling all determinants arising from the f^N multiplet. The trend of the reduction potentials along the series of early actinides was correct; however, the neglect of

Table 8 Comparison between the RASSI-SO (variation-perturbation) and EPCISO results on the $Np^{VI}(OH)_2$ and $Np^{V}(OH)_2$ complexes in the precursor state geometry (cf. Ref. [84])

Code	Fragment	States for which the orbitals are optimized	SO lowering of the GS (kJ/mol)
RASSI-SO	$Np(V)(OH)_2^-$	GS + excited states	79.5
EPCISO (no singles)	$Np(V)(OH)_2^-$	GS	71.5
EPCISO (with singles)	$Np(V)(OH)_2^-$	GS	82.3
EPCISO (no singles)	$Np(V)(OH)_2^-$	GS + excited states	79.9
EPCISO (with singles)	$Np(V)(OH)_2^-$	GS + excited states	81.0
RASSI-SO	$Np(VI)(OH)_2$	GS + excited states	33.3
EPCISO (no singles)	$Np(VI)(OH)_2$	GS	18.0
EPCISO (with singles)	$Np(VI)(OH)_2$	GS	32.0
EPCISO (no singles)	$Np(VI)(OH)_2$	GS + excited states	33.3
EPCISO (with singles)	$Np(VI)(OH)_2$	GS + excited states	35.0

Values taken from Ref. [85]

outer-sphere solvation effects results in reduction potentials that are overestimated by as much as 2–3 V.

Outer- and inner-sphere electron self-exchange reactions such as

$$MO_2^{2+} + M^*O_2^+ \rightleftharpoons M^*O_2^{2+} + MO_2^+ \quad (21)$$

were studied by Privalov et al. [84] and Macak et al. [45] in order to determine rate constants and activation energies, in this case the reactants and products are the same, therefore $\Delta G^\circ = 0$. However, it is important to include spin-orbit effects when there are open *f*-shells in the complexes. The spin-orbit effect was calculated using both the variation-perturbation method in the RASSI-SO module [3] of Molcas 5 [4] where the basis for the spin-orbit calculations was generated from multistate RASSCF calculations with equal weight on all configurations, and the spin-orbit CI method EPCISO [5] where the CI space includes all *f* configurations plus singly-excited configurations strongly coupled to the latter. Since spin-orbit effects are localized on the actinide centers, one can divide the full complex into fragments, each containing a single actinyl unit and the bridge. Fromager et al. [85] tested the accuracy of this procedure on the inner-sphere complexes with hydroxide and fluoride bridges [Eqs. (4), (5) and (6)] at the variation-perturbation level. The fragment method is quite accurate but the total spin-orbit effect is underestimated by about 2 kJ/mol, as compared to the calculation on the full complex.

Fromager et al. [85] also addressed the questions of the importance of *jj* coupling, and spin-orbit relaxation (different spatial extensions of the spinors in a multiplet) in neptunyl(VI) and neptunyl(V). It is generally assumed that spin-orbit relaxation effects are small in the actinides, and Fromager et al. [85] investigated the validity of this assumption. They used two different methods to calculate the spin-orbit effect; a variation-perturbation method based on an LS coupled basis set consisting of the 5*f*-manifold, and a multireference single excitation spin-orbit CI using the 5*f* manifold as the reference. The spin-orbit CI is also based on the LS coupling scheme but in this case both the spin-orbit and the scalar relaxation effects are properly accounted for by the interaction with the singly excited states. The results are summarized in Table 8.

Two conclusions can be drawn from these results. First, the close agreement between the single excitation spin-orbit CI using ground-state and state-averaged orbitals shows that the spin-orbit CI is capable of reproducing the scalar (electrostatic) relaxation effects in the excited reference states with high accuracy. Second, the close agreement between the single excitation spin-orbit CI and the variation-perturbation results (obtained with state-averaged orbitals) shows that spin-orbit relaxation effects are small. This indicates that *jj*-coupling effects are small for actinides, and presumably also for other transition elements, with open shells with high *l*-values [86]. Finally, it is important to underline that the spin-orbit CI method has some practical advantages compared to the variation-perturbation method because there is no need to use state-averaged orbitals, which are often difficult to obtain.

6 Thermodynamics of chemical reactions

Quantum chemistry offers the possibility to discuss the microscopic basis for chemical thermodynamics, that is to interpret macroscopic events in molecular terms. The link is provided by statistical thermodynamics through the molecular partition functions. This requires accurate information on the total electronic energy, and the vibration / rotation energy levels for reactants and products. The accuracy of the entropy calculations depends on the accuracy of the vibration energy levels. Analytical vibration frequencies are usually available only in gas phase and in general agree well with experimental values, cf. Privalov et al. [50]; the rotation frequencies in gas phase are calculated from the moments of inertia obtained in the geometry optimization. In "structured" solvents like water, free rotation is severely restricted and it seems reasonable to neglect rotation contributions. The contribution of translation and even its definition is less clear in a solvent [48].

A comparison of QM calculations of the vibration energy levels for small actinide molecules in gas phase indicate that the frequencies are not strongly dependent on the QM method used as discussed in Ref. [51]. Low-frequency modes make the largest contributions to the molecular partition functions, e.g. those describing hydrogen bond interactions between

solute and solvent. It seems unlikely that ab initio methods will be able to describe these accurately and to calculate accurate entropies for solutes in aqueous solution. However, the situation might well be different for entropies of reaction, provided that the systematic errors in the frequency calculation and the effect of the solvent compensate one another in the product and reactant. The only way to ascertain if this is the case or not, is to make comparisons with experimental data; Vallet et al. [48] have given examples that indicate that some compensation does indeed take place.

The electronic energy of reaction and the contribution from solvation are much smaller than the total energy of reactants and products, and it is necessary for systematic errors to balance in order to have reliable values for chemical reactions. In this section we shall discuss how this can be achieved and also the effect of different approximations on the thermodynamics of chemical reactions exemplified by

$$a\mathrm{A} + b\mathrm{B} \rightarrow c\mathrm{C} + d\mathrm{D}, \tag{22}$$

where charges have been omitted for simplicity. The reactants and products in complex formation reactions are often charged species. In order to have reasonably accurate values for the thermodynamics of reaction (22) in solution it is necessary that the systematic errors compensate one another. As discussed in Sect. 3.3, this is difficult to achieve if we treat each reactant and product separately; ions with different charge and different size will have widely different solvation energies. Even if the systematic error in the solvation energy for the reaction is most likely smaller than the accumulated error in each reactant and product, it still results in estimated thermodynamic quantities that differ widely from experimental data. Complex formation reactions involve the replacement of a ligand, usually water, in the first coordination sphere with a "free" ligand. A better approach to calculate the thermodynamics of the reaction is then to divide reaction (22) into two parts, as shown in Eqs. (8) and (9) where the first part is the formation of an outer-sphere complex that can be described using the Fuoss equation [46, 47] and the second an intramolecular reaction that is described using QM, as discussed in Sect. 3.3. In the calculation of the Gibbs energy of reactions for reaction (8) and (9), Vallet et al. [48] used gas phase vibration frequencies to calculate the entropies for reactants and products and the enthalpy of reaction. It is of interest to note that the calculated entropy and enthalpy of reaction for the two-step model are also in better agreement with the experimental observations than the calculation based on Eq. (7). The method outlined by Vallet et al. has limitations as discussed in Sect. 4.2, a second example is shown in Fig. 2, where the outer sphere oxalate ligand abstracts proton from coordinated water.

It is well known that there are large similarities in the chemistry of the actinides if they are in the same oxidation state. One can then use experimental data for one actinide, e.g. thorium or uranium to calibrate QM calculations and in this way obtain information on the variation of chemical properties throughout the actinide series. This has important practical implications because it makes it possible to estimate thermodynamic data for elements that are highly toxic and difficult and expensive to study experimentally.

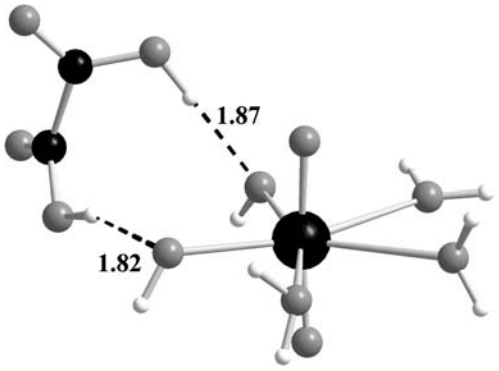

Fig. 2 Perspective view of the structure of $[UO_2(H_2O)_5^{2+}]$ $(oxalate)^{2-}$ that shows double proton abstraction from the oxalate group. The geometries have been optimized at the HF level in gas-phase. The *dashed line* indicates hydrogen bond interactions. Bond distances are in Å ngström

7 Conclusions

In this article we have presented a critical discussion of published computational studies of actinides chemistry in gas phase and in solution. The most important criteria to benchmark theoretical methods is the extent to which systematic errors affect the computed physico-chemical quantities such as electronic energy, structures, energy levels and solvation. The systematic errors in chemical reactions depend critically on cancellation of systematic errors between reactants and products and this is strongly influenced by the chemical model used to describe the "real" systems. In complex formation and ligand-substitution reactions in actinyl complexes, where weak labile bonds are broken / formed, strong correlation effects are localized in the axial "actinyl" triple bonds. Since the axial oxygen atoms do not participate in the ligand exchange process, errors in the energy of reaction and activation energies, induced by the choice of basis set, correlation effects, spin-orbit contributions, essentially compensate each other along the reaction path. However, whenever affordable, the geometry optimization should be made at the MP2 level in order to achieve better comparison with experimental structure data. Previous studies and the discussion in this review demonstrate that static correlation of the near degeneracy type is not important in actinyl complexes and that the MP2 method is therefore well suited to describe correlation; these results refute the claims in Ref. [82]. Single point MP2 energies, based on both HF and MP2 optimized geometries give very similar reaction energies. Redox and electron-transfer reactions imply significant rearrangement of the electron density at or close to the actinide centre. This makes it necessary to describe electron correlation by using more elaborated post-HF methods (CCSD(T), MRCI, CASPT2) than that used for complex formation / ligand-exchange reactions. Here, most density functionals presently fail because of the

wrong behavior at long-distance, which bias the description of charge-transfer and redox reactions.

Solute–solvent interactions have a profound influence on the relative stability of different isomers and on the energetics of chemical reactions. At present most studies have been made using continuum models, but there are some studies made using combined QM/MM methods. In the examples available the two approaches give similar results. However, both methodological improvements and benchmarks have to be considered in the future.

Li and Fu (Ref [87] and references therein) have suggested that a factor of 0.5 is missing in front of the right hand side of Eq. (3); however, this is of little consequence in the applications discussed in the present review.

Acknowledgements This study has been made within the scope of the EU network ACTINET. It has been supported by a generous grant from the Trygger Foundation. The Laboratoire de Physique des Lasers, Atomes et Molecules is Unité Mixte de Recherche Mixte du CNRS. The Centre d'Etudes et de Recherches Lasers et Applications is supported by the Ministère chargé de la Recherche, the Région Nord-Pas de Calais, and the Fonds Européen de Développement Economique des Régions. We also gratefully acknowledge a generous grant from the Swedish Nuclear Fuel and Waste Management Company (SKB).

References

1. Douglas M, Kroll NM (1974) Ann Phys (NY) 82:89–155
2. Hess BA (1986) Phys Rev A 33:3742–3748
3. Malmqvist PÅ, Roos BO, Schimmelpfennig B (2002) Chem Phys Lett 357:230–240
4. Karlström G, Lindh R, Malmqvist P-Å, Roos BO, Ryde U, Veryazov V, Widmark P-O, Cossi M, Schimmelpfennig B, Neogrady P, Seijo L (2003) Comput Mater Sci 28:222–239
5. Vallet V, Maron L, Teichteil C, Flament J-P (2000) J Chem Phys 113:1391–1402
6. Heß B A, Marian CM, Wahlgren U, Gropen O (1996) Chem Phys Lett 251:365–371
7. Schimmelpfennig B (1996) AMFI, an atomic mean-field integral program. Stockholm University, Stockholm
8. Pyykkö P (1987) Inorg Chim Acta 139:243–245
9. Küchle W, Dolg M, Stoll H (1994) J Chem Phys 100:7535–7542
10. Küchle W (1993) Diplomarbeit
11. Ismail N, Heully J-L, Saue T, Daudey J-P, Marsden C (1999) Chem Phys Lett 300:296–302
12. Vallet V, Schimmelpfennig B, Maron L, Teichteil C, Leininger T, Gropen O, Grenthe I, Wahlgren U (1999) Chem Phys 244:185–193
13. García-Hernández M, Lauterbach C, Krüger S, Matveev A, Rösch N (2002) J Comput Chem 23:834–846
14. Batista ER, Martin RL, Hay PJ, Peralta JE, Scuseria GE (2004) J Chem Phys 121:2144–2150
15. Straka M, Kaupp M (2005) Chem Phys 311:45–56
16. Hay PJ, Wadt WR, Kahn LH (1979) J Chem Phys 71:1767–1779
17. Hay PJ, Wadt WR (1985) J Chem Phys 82:270–283
18. Hay PJ (1983) J Chem Phys 79:5469–5482
19. Hay PJ, Martin RL (1998) J Chem Phys 109:3875–3881
20. Tsushima S, Uchida Y, Reich T (2002) Chem Phys Lett 357:73–77
21. Purvis III GD, Bartlett RJ (1982) J Chem Phys 76:1910–1918
22. Raghavachari K, Trucks GW, Pople JA, Head-Gordon M (1989) Chem Phys Lett 157:479–483
23. Watts JD, Gauss J, Bartlett RJ (1993) J Chem Phys 98:8718–8733
24. Langhoff SR, Davidson ER (1974) Int J Quantum Chem 8:61–72
25. Gdanitz RJ, Ahlrichs R (1988) Chem Phys Lett 143:413–420
26. Andersson K, Malmqvist P-Å, Roos BO, Sadlej AJ, Wolinski K (1990) J Phys Chem 94:5483–5488
27. Andersson K, Malmqvist P-Å, Roos BO (1992) J Chem Phys 96:1218–1226
28. Weigend F, Häser M Theor Chim Acc (1997) 97:331–340
29. Weigend F, Häser M, Patzelt H, Ahlrichs R (1998) Chem Phys Lett 294:143–152
30. Becke, AD (1993) J Chem Phys 98:5648–5652
31. Tomasi J, Persico M (1994) Chem Rev 94:2027–2094
32. Cramer CJ, Truhlar DG (1999) Chem Rev 99:2161–2200
33. Warshel A, Levitt MJ (1976) Mol Biol 103:227–249
34. Singh UC, Kollman PA (1986) J Comput Chem 7:718–730
35. Bash PA, Field MJ, Karplus M (1987) J Am Chem Soc 109:8092–8094
36. Woo TK, Cavallo LC, Ziegler T (1998) Theor Chim Acc 100:307–313 and references therein
37. Infante I, Visscher L (2004) J Comput Chem 25:386–392
38. Yang T, Tsushima S, Suzuki A (2001) J Phys Chem A 105:10439–10445
39. Yang T, Tsushima S, Suzuki A (2002) Chem Phys Lett 360:534–542
40. Elrod MJ, Saykally RJ (1994) Chem Rev 94:1975–1997
41. Car R, Parrinello M (1985) Phys Rev Lett 55:2471–2474
42. Warshel A, Karplus M (1972) J Am Chem Soc 94:5612–5625
43. Vallet V, Wahlgren U, Schimmelpfennig B, Moll H, Szabó Z, Grenthe I (2001) Inorg Chem 40:3516–3525
44. Cossi M, Barone V (2000) J Chem Phys 112:2427–2435
45. Macak P, Fromager E, Privalov T, Schimmelpfennig B, Grenthe I, Wahlgren U (2005) J Phys Chem A 109:4950–4956
46. Fuoss RM (1958) J Am Chem Soc 80:5059–5061
47. Margerum DW, Cayley GR, Pagenkopf GK (1978) In: Martell AE (ed.) Coordination chemistry, vol. 2. ACS Monograph 174, Washington DC, pp 1–220
48. Vallet V, Wahlgren U, Grenthe I (2003) J Am Chem Soc 125: 14941–14950
49. Craw JS, Vincent MA, Hillier IH, Wallwork AL (1995) J Phys Chem 99:10181–10185
50. Privalov T, Schimmelpfennig B, Wahlgren U, Grenthe I (2003) J Phys Chem A 107:587–592
51. Schimmelpfennig B, Privalov T, Wahlgren U, Grenthe I (2003) J Phys Chem A 107:9705–9711
52. Zhou M, Andrews L, Ismail N, Marsden C (2000) J Phys Chem A 104:5495–5502
53. Weinstock B, Goodman GL (1965) Adv Chem Phys 9:169
54. Han Y-H, Hirao K (2000) J Chem Phys 113:7345–7350
55. Bergner A, Dolg M, Küchle W, Stoll H, Preuss H, (1993) Mol Phys 80:1431–1441
56. Schäfer A, Huber C, Ahlrichs R (1994) J Chem Phys 100:5829–5935
57. Huzinaga S (1965) J Chem Phys 42:1293–1302
58. Schäfer A, Horn H, Ahlrichs R (1992) J Chem Phys 97:2571–2577
59. Wahlgren U, Moll H, Grenthe I, Schimmelpfennig B, Maron L, Vallet V, Gropen O (1999) J Phys Chem A 103:8257–8264
60. Vallet V, Wahlgren U, Schimmelpfennig B, Szabó Z, Grenthe I (2001) J Am Chem Soc 123:11999–12000
61. Gagliardi L, Grenthe I, Roos BO (2001) Inorg Chem 40:2976–2978
62. Gagliardi L, Roos B. O. (2002) Inorg Chem 41:1315–1319
63. Vallet V, Moll H, Wahlgren U, Szabó Z, Grenthe I (2003) Inorg Chem 42:1982–1993
64. Docrat TI, Mosselmans JFW, Charnock JM, Whiteley MW, Collison D, Livens FR, Jones C, Edmiston MJ (1999) Inorg Chem 38:1879–1882
65. Pyykkö P, Li J, Runeberg N (1994) J Phys Chem 98:4809–4813
66. Clark DL, Conradson SD, Ekberg SA, Hess NJ, Neu MP, Palmer PD, Runde W, Tait CD (1996) J Am Chem Soc 118:2089–2090
67. Hay PJ, Martin RL, Schreckenbach G (2000) J Phys Chem A 104:6259–6270
68. Martínez JM, Pappalardo RR, Sánchez-Marcos E, Mennucci B, Tomasi J (2002) J Phys Chem B 106:1118–1123
69. Martínez JM, Pappalardo RR, Sánchez-Marcos E (1997) J Phys Chem A 101:4444–4448
70. Van Lenthe E, Snijders JG, Baerends EJ (1996) J Chem Phys 105:6505–6516

71. Matsika S, Pitzer RM (2000) J Phys Chem A 104:4064–4068
72. Clavaguéra-Sarrio C, Vallet V, Maynau D, Marsden CJ (2004) J Chem Phys 121:5312–5321
73. Roos BO, Widmark P-O, Gagliardi L (2003) Faraday Discuss 124:57–62
74. Vallet V, Maron L, Schimmelpfennig B, Leininger T, Teichteil C, Gropen O, Grenthe I, Wahlgren U (1999) J Phys Chem A 103:9285–9289
75. Moskaleva LV, Krüger S, Spröl A, Rösch N (2004) Inorg Chem 43:4080–4090
76. Tsushima S, Yang T, Suzuki A (2001) Chem Phys Lett 334:365–373
77. Ismail N (2000) Thesis, Etude théorique de l'ion uranyle et de ses complexes et dérivés, Université Paul Sabatier de Toulouse
78. Hehre WJ, Ditchfield R, Pople JA (1972) J Chem Phys 56:2257–2261
79. Bouteiller Y, Mijoule C, Nizam M, Barthelat JC, Daudey JP, Pelissier M (1988) Mol Phys 65:295–312
80. Dunning TH, Hay PJ (1976) Modern theoretical chemistry, Plenum, New York, pp 1–28
81. Clavaguéra-Sarrio C, Brenner V, Hoyau S, Marsden CJ, Millié P, Dognon J-P (2003) J Phys Chem B 107:3051–3060
82. Rotzinger FP (2005) Chem Rev 105:2003–2037
83. Vallet V, Privalov T, Wahlgren U, Grenthe I (2004) J Am Chem Soc 126: 7766–7767
84. Privalov T, Macak P, Schimmelpfennig B, Fromager E, Grenthe I, Wahlgren U (2004) J Am Chem Soc 126:9801–9808
85. Fromager E, Vallet V, Schimmelpfennig B, Macak P, Privalov T, Grenthe I, Wahlgren U (2005) J Phys Chem 109:4957–4960
86. Matsika S, Pitzer RM (2001) J Phys Chem A 105:637–645
87. Li X-Y, Fu K-X (2004) J Comp Chem 25:500–509